Nuclear spin relaxation rate of magnetic impurities in quantum Hall effect systems

P. Dahan*
P.E.R.I Physics and Engineering Research Institute, School of Engineering at Ruppin Academic Center, Emek-Hefer 40250, Israel

I. D. Vagner
Grenoble High Magnetic Field Laboratory Max-Planck-Institut für Festkörperforschung and CNRS, Boîte Postale 166, 38042, Grenoble Cedex 09, France
and Research Center for Quantum Communication Engineering, Department of Communication Engineering, Holon Academic Institute of Technology, 52 Golomb Str., Holon 58102, Israel
(Received 7 April 2005; published 22 September 2005)

The magnetic field dependence of the local phonon-assisted nuclear spin relaxation rate in two-dimensional electron systems with magnetic impurities is studied theoretically. For weak- and strong-scattering limits under strong magnetic fields we show that the magnetic field dependence of T_1^{-1} exhibits giant spikes, due to the energy matching of the electron Zeeman splitting with the energy spacing between the vibrational mode energies. The localized mode is created by the lattice distortion around the impurity. This resonance phenomenon could be used as a local probe for studying the localized vibrational modes and their coupling to electrons and for the resonant manipulation of the nuclear spin qubits. Possible applications to the future nuclear spin-qubit based quantum computation and communication devices are discussed.

DOI: 10.1103/PhysRevB.72.115328 PACS number(s): 76.60.−k, 71.55.−i

I. INTRODUCTION

The unique properties of two-dimensional electron systems (2DES's) in strong magnetic fields together with their potential applications in microelectronics put these systems among the hottest topics in the studies of strongly correlated electron systems. The nuclear and electron spin states in heterostructures, quantum wires, dots, and similar nanostructures have attracted much attention in recent years. Recent progress in quantum Hall effect (QHE) physics[1] is closely connected with the rich world of the hyperfine interaction between nuclear and electron spins in quantum Hall[2,3] and nanosystems.[4–7]

Various types of excitons[8–10] and collective topological excitations (Skyrmions) (Ref. 11) arise due to the interplay between orbital and spin degrees of freedom in the integer quantum Hall effect (IQHE). The fractional quantum Hall effect is a manifestation of unusual electron correlations, resulting in unusual quantum statistics of 2DES's. The nuclear spin subsystem being coupled by hyperfine interactions to the electron spin subsystem may be extremely operative in providing microscopic information on the correlated electronic states.[2,12] The hyperfine field of nonequilibrium nuclear spins may result in an electron Zeeman splitting equivalent to several tesla of external magnetic field,[13] which can even produce new, dynamic, low-dimensional systems.[5] Experiments indicate very long spin decoherence times and small nuclear spin transition rates.[3]

These promising results have motivated proposals for information processing based on nuclear and electron spins which might lead to the realization of nuclear-spin-based quantum memory[14] and computing.[15–19]

Nuclear and electron spin can be manipulated better in a coherent way when they can be isolated from the surrounding environment. One of the measures for such isolated systems is the strength of the coupling to the environment which depends on the spin-flip transition rate.

The simultaneous electron-nuclear spin flip, caused by the contact (Fermi) interaction, in QHE systems and nanosystems with the discret electron spectrum is severely restricted, at low temperatures, by energy conservation.[2] This follows from the fact that the electron Zeeman splitting is orders of magnitude larger than the nuclear Zeeman splitting. The electron-nuclear flip-flop process in these systems can take place, therefore, when external factors, such as impurities, phonons, edge states, etc., couple the electron to an external energy bath.[2]

An effective mechanism in QHE systems is the phonon-assisted electron-nuclear flip-flop.[20]

Unlike the case of 2D extended Landau states we deal here with a substitutional impurity. The impurity scattering is responsible for the broadening of Landau levels and the creation of localized states in 2DES's. The genesis of the bound states due to short-range potential scattering was described in Refs. 21 and 22 The role of magnetic impurities in the formation of the excitation spectrum in 2DES's was discussed previosly in our previous paper.[23] We have shown there that the resonance impurity scattering results in the appearance of bound Landau states with zero moment between the Landau subbands. Since the resonance scattering is spin selective, it results in a strong spin polarization of Landau states. The nuclear spin impurity interacts, therefore, only with these discrete bound Landau states.

Using similar arguments one may expect resonant enhancement of the phonon-assisted flip-flop processes, since the lattice distortion around the defect creates localized phonons in the phonon band gap. These localized phonons may be considered as breathing modes acting up to a few nearest neighbors in a shell around the impurity.[24]

In this paper we calculate the magnetic field dependence of the nuclear spin relaxation rate (NSR) T_1^{-1} of nuclei belonging to magnetic impurities placed in the two-dimensional electron system under strong external magnetic

fields. The cases of weak- and strong-scattering limits are treated in detail. It is found that only resonance transitions are allowed to occur, whenever electron magnetic gaps fit the vibrational-mode energies. This spectral structure can be used as a probe for studying the localized vibrational-mode frequency and the electron-phonon coupling for various transition-metal impurities.

The hyperfine contact (Fermi) interaction with the localized Landau state is calculated here for the first time. Estimates for the Fe impurity in GaAs in the framework of our model are given.

II. GENERAL MODEL

Let us consider the model of a two-dimensional electron gas in a quantizing magnetic field which interacts with the impurity nuclear spins and phonons. Here we discuss the nuclear spin relaxation of the impurity via a hyperfine interaction with localized Landau states. The Hamiltonian of such a system is

$$H = H_e + H_{ph} + H_{int}. \tag{1}$$

Here H_e is the impurity Hamiltonian in a magnetic field B parallel to the z axis,

$$H_e = H_0 + V_d(\mathbf{r} - \mathbf{R}_0), \tag{2}$$

where

$$H_0 = \frac{1}{2m^*}\left(\mathbf{P} + \frac{e}{c}\mathbf{A}\right)^2 + V(z) \tag{3}$$

describes the motion of an electron in the conduction band with the effective mass m^*, confined in the z direction by the potential $V(z)$. $V_d(\mathbf{r}-\mathbf{R}_0)$ is the substitutional impurity potential at a site $\mathbf{R}_0$. It is shown[23] that this scattering results in the appearance of bound Landau states with zero moment between the Landau subbands. The resonance scattering is spin selective, and it results in a strong spin polarization of Landau states, as well as in a noticeable magnetic field dependence of the g factor and crystal field splitting of impurity d levels. The H_{ph} term is the Hamiltonian of the phonon system.

Two interaction terms are considered here to be responsible for relaxing a polarized nuclear spin of the impurity by flipping an electron spin. This spin flipping is caused by the contact hyperfine interaction described by

$$H_{hf} = \frac{2}{3}\mu_0 g_e \mu_B g_N \beta_N \mathbf{I}\cdot\mathbf{S}\,\delta(\mathbf{r}-\mathbf{R}_0), \tag{4}$$

where $\mathbf{I}$ and $\mathbf{s}$ are the nuclear and electron spins, respectively, g_e and g_N are the electron and the nuclear (N) g value, and μ_B and β_N are the electron and nuclear Bohr magnetons.[12,13] For free electrons, in the absence of the quantized magnetic field, the change in energy accompanying a spin flip caused by the hyperfine scattering is compensated for by an appropriate change in its kinetic energy. In our system of the bound electron with a discrete energy spectrum, no hyperfine-induced transition will occur because the energy required for the electron spin flip is not available. Therefore, the nuclear spin relaxation in our system requires taking into account the electron coupling to the lattice vibrations.

The electron-phonon interaction contains two parts,

$$H_{eph} = H^c_{eph} + H^{loc}_{eph}, \tag{5}$$

where H^c_{eph} is the electron interaction with the continues lattice phonons and H^{loc}_{eph} is the electron interaction with the localized phonons coupled to the localized magnetic impurities. Since the localized Landau states are s functions ($m=0$), the nuclear spin of the impurity interacts mainly with these states. In our case, we would expect, therefore, the important interaction to be with the localized phonons acting as a breathing-mode distortion up to a few nearest-neighbor shells around the impurity.[24]

The electron phonon interaction in the occupation number formalism can be written in the form

$$H^{loc}_{eph} = \sum_{\Gamma M} A^{\lambda',\lambda\sigma}_{\Gamma M}\rho^{\Gamma M}_{\lambda',\lambda}(a^\dagger_{\Gamma M} + a_{\Gamma M}), \tag{6}$$

where $a^\dagger_{\Gamma M}$ and $a_{\Gamma M}$ are, respectively, the phonon creation and annihilation operators for the ΓM vibration modes. $A^{\lambda',\lambda\sigma}_{\Gamma M}$ is the electron-phonon coupling having dimension of energy for the Γ irreducible representation for lattice distortions. $\rho^{\Gamma M}_{\lambda,\lambda'}$ is the dimensionless tensor whose upper indices relate to the lattice coordinates while the lower indices relate to the electrons, $\lambda = n\gamma\nu$. $\gamma\nu$ is the localized electron in the nth Landau level with the energy E^σ_{bn}.[23] Here $\gamma = e, t_2$ determines the irreducible representation of the crystalline point group for the d states and ν enumerates lines of these irreducible representations. The point group T_d is implied throughout this paper. Thus for T_d symmetry there are four nearest neighbors that give rise to the vibrational modes $\Gamma = A_1 + E + 2T_2 + T_1$.[25] The electron-phonon coupling is described by

$$A^{\lambda',\lambda\sigma}_{\Gamma M} = \frac{1}{\alpha_\Gamma}\langle\Phi^{(n')\sigma}_{i\gamma'\nu'}|V_{\Gamma M}(\mathbf{r})|\Phi^{(n)\sigma}_{i\gamma\nu}\rangle, \tag{7}$$

where $\alpha_\Gamma = \sqrt{M(\Gamma)\omega_\Gamma/\hbar}$ and $M(\Gamma)$ and ω_Γ are the reduced mass and frequency of the Γ vibrational mode, respectively. $V_{\Gamma M}(\mathbf{r})$ is the linear term of the interaction energy of the crystal potential. $\Phi^{(n)}_{i\gamma\nu}$ is the wave function of the localized electron obtained by solving the Hamiltonian (2) of the electron system with energy E^σ_{bn} (see Ref. 23).

There are two possible channels for relaxing the polarized nuclear spin of the impurity with a phonon-assisted process; one of them is presented in Fig. 1.

The transition rate is calculated by

$$W(T_1) = \sum_{if} W_{if} N_\Gamma f_{n\uparrow}(1 - f_{n'\downarrow}), \tag{8}$$

where the Fermi function $f_{n\sigma} = (e^{\beta(E^\sigma_{bn}-\mu)}+1)^{-1}$ and the Bose function $N_\Gamma(\beta\omega) = (e^{\beta\hbar\omega_\Gamma}-1)^{-1}$ are the occupation probabilities for both electron and phonons, respectively. $\beta = 1/k_B T$, μ is the chemical potential, and n and n' are the initial and final electron states. To obtain the transition probability W_{if} we employ second-order perturbation theory:

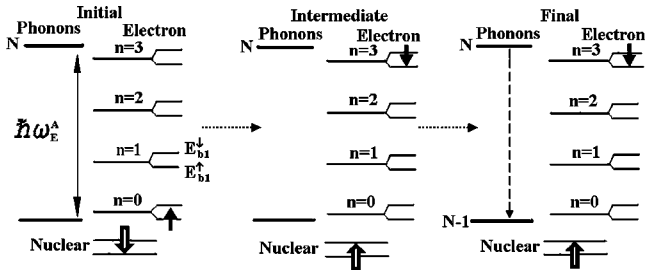

FIG. 1. A schematic diagram for processes in the phonon-assisted NSR mechanism for relaxing the polarized nuclear spin under the QHE condition. The dashed line represents the phonon. The inital, intermediate, and final states of each process are denoted accordingly. The phonon energy and the electronic and nuclear Zeeman energy splittings are drawn out of scale.

$$W_{if} = \frac{2\pi}{\hbar}\left|\sum_m \left[\frac{\langle f|H_{eph}|m\rangle\langle m|H_{hf}|i\rangle}{E_i - E_m} + \text{c.c.}\right]\right|^2 \delta(E_i - E_f), \tag{9}$$

where i, m, and f denote, respectively, the general wave function $\Psi = |\mathbf{I}\rangle|\mathbf{s}\rangle|N_{\Gamma M}\rangle\Phi_{i\gamma\mu}^{(n)\sigma}$ of the initial, intermediate, and final states. Here $|\mathbf{I}\rangle$ and $|\mathbf{s}\rangle$ are the nuclear and electron spins functions and $|N_{\Gamma M}\rangle$ are the phonon states of the harmonic oscillator energy. $N_{\Gamma M}$ denotes the number of localized phonons with angular frequency ω_Γ.

First consider the initial intermediate and final energies

$$E_i = E_{bn}^{\uparrow} + \frac{1}{2}\gamma_n\hbar B + \hbar\omega_\Gamma\left(N + \frac{1}{2}\right),$$

$$E_f = E_{bn'}^{\downarrow} - \frac{1}{2}\gamma_n\hbar B + \hbar\omega_\Gamma\left(N' + \frac{1}{2}\right),$$

$$E_m = E_{bn''}^{\downarrow} - \frac{1}{2}\gamma_n\hbar B + \hbar\omega_\Gamma\left(N'' + \frac{1}{2}\right) \text{ for channel } A,$$

$$E_m = E_{bn''}^{\uparrow} + \frac{1}{2}\gamma_n\hbar B + \hbar\omega_\Gamma\left(N'' + \frac{1}{2}\right) \text{ for channel } B, \tag{10}$$

where $E_{bn}^{\uparrow,\downarrow}$ is the renormalized bound Landau states[23] and $\frac{1}{2}\gamma_n\hbar B$ is the nuclear spin energy splitting.

Inserting the interaction terms (4) and (6) into the transition probability (9) and combining with Eq. (8) we obtain the following expression for the relaxation rate:

$$W(T_1) = \frac{\pi(A')^2}{2\hbar}\sum_{\Gamma M N_\Gamma \lambda'\lambda''\lambda} \frac{R}{Q}\delta(E_{bn}^{\uparrow} - E_{bn'}^{\downarrow} + \hbar\omega_\Gamma), \tag{11}$$

where $A' = \frac{2}{3}\mu_0 g_e \mu_B g_N \beta_N$. Here R is the amplitude of the transition probability given by

$$R = \frac{R_{\Gamma M\downarrow}^{\lambda'\lambda''\lambda}}{(E_{bn}^{\uparrow} - E_{bn''}^{\downarrow})^2} + \frac{R_{\Gamma M\uparrow}^{\lambda'\lambda''\lambda}}{(E_{bn}^{\uparrow} - E_{bn''}^{\uparrow} + \hbar\omega_\Gamma)^2}, \tag{12}$$

where $R_{\Gamma M\downarrow}^{\lambda'\lambda''\lambda} = |A_{\Gamma M}^{\lambda',\lambda''\downarrow}\rho_{\lambda',\lambda''}^{\Gamma M} S^{\lambda''\downarrow,\lambda\uparrow}|^2$ for channel A and $R_{\Gamma M\uparrow}^{\lambda'\lambda''\lambda} = |S^{\lambda'\downarrow,\lambda''\uparrow} A_{\Gamma M}^{\lambda'',\uparrow}\rho_{\lambda'',\lambda}^{\Gamma M}|^2$ for channel B. The matrix elements of the Fermi contact interaction are

$$S^{\lambda''\downarrow,\lambda\uparrow} = \langle\Phi_{i\gamma''\mu''}^{(n'')\downarrow}|\delta(\mathbf{r})|\Phi_{i\gamma\mu}^{(n)\uparrow}\rangle. \tag{13}$$

$Q^{-1} = N_\Gamma f_{n\uparrow}(1 - f_{n'\downarrow})$ can be written as

$$Q^{-1} = \frac{\exp\left\{\frac{\beta}{2}(E_{bn'}^{\downarrow} - E_{bn}^{\uparrow} - \hbar\omega_\Gamma)\right\}}{\sinh\frac{\beta}{2}\hbar\omega_\Gamma\left[\cosh f_\Gamma(E) + \cosh\frac{\beta}{2}(E_{bn'}^{\downarrow} - E_{bn}^{\uparrow})\right]}, \tag{14}$$

where $f_\Gamma(E) = (\beta/2)(E_{bn'}^{\downarrow} + E_{bn}^{\uparrow} - 2\mu)$.

Using the energy conservation $\delta(E_{bn}^{\uparrow} - E_{bn'}^{\downarrow} + \hbar\omega_\Gamma)$ the relaxation rate (11) becomes

$$W(T_1) = \frac{\pi(A')^2}{2\hbar}\sum_{\Gamma M N_\Gamma \lambda'\lambda''\lambda} R \times \frac{\delta(E_{bn}^{\uparrow} - E_{bn'}^{\downarrow} + \hbar\omega_\Gamma)}{\sinh\frac{\beta}{2}\hbar\omega_\Gamma\left[\cosh f_\Gamma(E) + \cosh\frac{\beta}{2}(\hbar\omega_\Gamma)\right]}, \tag{15}$$

where $f_\Gamma(E) = \beta\left(E_{bn}^{\uparrow} - \mu + \frac{1}{2}\hbar\omega_\Gamma\right)$.

To complete the calculation of the relaxation time we express the energies E_{bn}^{σ} in Eqs. (12) and (14). In the limit of a strong magnetic field $|\varepsilon_{b0}|l_B^2 \ll 1$ the energy spectrum of the localized states is

$$\varepsilon_{b\sigma}^{(n)} = \varepsilon_\sigma^{(n)} - \frac{2\delta_{n+1}}{l_B^2}, \tag{16}$$

where $\delta_n = |\ln 2e^{\psi(n)}/|\varepsilon_{b0}|l_B^2|^{-1} \ll 1$,[21] ε_{b0} is the energy of the electron, bound by the attractive potential V, l_B is the the magnetic length, and $\psi(n)$ is the digamma function. This yields the energy to be

$$E_{bn}^{\sigma} = \hbar\omega_c\left(n + \frac{1}{2} - \delta_{n+1}\right) + \sigma g_{eff}\mu_B B. \tag{17}$$

The effective g factor g_{eff} of the bound electron will be considered here as field independent (see Ref. 23 for a detailed calculation of the magnetic field dependence of the g factor in these systems). The energy difference becomes

$$E_{bn}^{\uparrow} - E_{bn''}^{\downarrow} = \hbar\omega_c(n - n'' + \Delta_{n''n}) - g_{eff}\mu_B B, \tag{18}$$

where $\Delta_{n''n} = \delta_{n''+1} - \delta_{n+1}$. Substituting $B = \tilde{n}\phi_0/x$, where x is the number of full bands, $\tilde{n} = N/L^2$ is the electrons density, and B/ϕ_0 is the Landau level degeneracy and using $\hbar\omega_c$

$=h^2\tilde{n}/2\pi m^* x$ the energy difference in Eq. (12) for channel A becomes

$$E^{\uparrow}_{bn} - E^{\downarrow}_{bn''} = \frac{\tilde{n}}{x}\left[\frac{h^2}{2\pi m^*}(n - n'' + \Delta_{n''n}) - g_{eff}\mu_B\phi_0\right]. \tag{19}$$

In a strong magnetic field limit, $\delta_n \ll 1$ and $\delta_{n''+1} - \delta_{n+1} = \Delta_{n''n} < 0$ so that $|n-n''| > |\Delta_{n''n}|$. Therefore

$$E^{\uparrow}_{bn} - E^{\downarrow}_{bn''} = \frac{\tilde{n}}{x}[-F_{n''n} - g_{eff}\mu_B\phi_0], \tag{20}$$

where $F_{n''n} = |(h^2/2\pi m^*)(n-n''+\Delta_{n''n})|$. Using the energy conservation $E^{\uparrow}_{bn} - E^{\downarrow}_{bn'} + \hbar\omega_\Gamma = 0$, the energy difference in Eq. (12) for channel B becomes

$$E^{\uparrow}_{bn} - E^{\uparrow}_{bn''} + \hbar\omega_\Gamma = \frac{\tilde{n}}{x}\left[\frac{h^2}{2\pi m^*}(n' - n'' + \Delta_{n''n'}) + g_{eff}\mu_B\phi_0\right],$$

$$E^{\uparrow}_{bn} - E^{\uparrow}_{bn''} + \hbar\omega_\Gamma = \frac{\tilde{n}}{x}[F_{n''n'} + g_{eff}\mu_B\phi_0], \tag{21}$$

where $F_{n''n'} = (h^2/2\pi m^*)(n' - n'' + \Delta_{n''n'})$.

Inserting Eqs. (20) and (21) and the energy conservation

$$\delta(E^{\uparrow}_{bn} - E^{\downarrow}_{bn'} + \hbar\omega_\Gamma) = \frac{1}{\hbar\omega_c}\delta\left(n - n' + \frac{2\pi m^*_e \hbar\omega_\Gamma}{h^2\tilde{n}}x - \frac{2\pi m^*_e g_{eff}\mu_B\phi_0}{h^2} - \Delta_{nn'}\right)$$

into Eq. (15) the transition rate becames

$$W(T_1) = \frac{\pi(A')^2}{2\hbar}\sum_{\Gamma M n n' n''}\frac{2\pi m^*_e}{h^2}\frac{x^3}{\tilde{n}^3} \times R\frac{1}{\sinh\frac{\beta}{2}\hbar\omega_\Gamma\left[\cosh f_\Gamma(x) + \cosh\frac{\beta}{2}(\hbar\omega_\Gamma)\right]}, \tag{22}$$

provided the final state n' satisfies

$$n' = n + \frac{2\pi m^*\hbar\omega_\Gamma}{h^2\tilde{n}}x - \frac{2\pi m^* g_e\mu_B\phi_0}{h^2} - (\delta_{n+1} - \delta_{n'+1}). \tag{23}$$

The amplitude R, Eq. (12), becomes

$$R = \frac{R_{\Gamma M\downarrow}}{(-F_{n''n} - g_{eff}\mu_B\phi_0)^2} + \frac{R_{\Gamma M\uparrow}}{(F_{n''n'} + g_{eff}\mu_B\phi_0)^2}.$$

$R_{\Gamma M\sigma}$ will be presented in detail in Sec. IV. Here

$$f_\Gamma(x) = t\left\{\left[A\left(n + \frac{1}{2} - \delta_{n+1}\right) - 1\right]\frac{1}{x} - \mu^*\right\} + \frac{\beta}{2}\hbar\omega_\Gamma, \tag{24}$$

with the parameters A, t, and μ^* defined by

$$t = \frac{1}{2}\beta g_{eff}\mu^e_B\tilde{n}\phi_0, \quad A = \frac{2\hbar e}{m^* c g_{eff}\mu^e_B}, \tag{25}$$

$$\mu^* = \frac{2\mu}{g_{eff}\mu^e_B\tilde{n}\phi_0}. \tag{26}$$

The dominant contribution of the transition rate, Eq. (22), obtained for n, n', and n'' leads to $F_{n''n}=0$—i.e., $n''=n$—and $F_{n''n'}=0$—i.e., $n''=n'$:

$$W(T_1) = D\sum_{\Gamma M n n'\sigma}\frac{(R_{\Gamma M\sigma})x^3}{\sinh\frac{\beta}{2}\hbar\omega_\Gamma\left[\cosh f_\Gamma(x) + \cosh\frac{\beta}{2}(\hbar\omega_\Gamma)\right]}, \tag{27}$$

where $D = 8\pi^3 m^*(\mu_0 g_N\beta_N)^2/9h^3\tilde{n}^3\phi_0^2$.

μ^* is defined for two different cases: for the case when ε_F is situated between Zeeman-split electron energy levels and for the case when ε_F is between two adjacent Landau levels. The magnetic field dependence of the chemical potential μ^* is calculated in the next section.

III. CHEMICAL POTENTIAL OSCILLATIONS

In order to calculate the transition rate $W(T_1)$ we are required to calculate the chemical potential $\mu(B)$ for two cases: $\varepsilon^{\downarrow}_{n_F} \leqslant \mu \leqslant \varepsilon^{\uparrow}_{n_F}$—i.e., ε_F between two Zeeman levels and $\varepsilon^{\downarrow}_{n_F} \leqslant \mu \leqslant \varepsilon^{\uparrow}_{(n_F+1)}$—i.e., ε_F between two Landau levels. We start with the normalization condition

$$N = \frac{BL^2}{\phi_0}\sum_{\sigma,n=0}^{\infty}\frac{1}{\exp\left\{\beta\left[\hbar\omega_c\left(n + \frac{1}{2}\right) + \frac{1}{2}\sigma g_e\mu^e_B B - \mu\right]\right\} + 1}, \tag{28}$$

and by using the definition for t, A, μ^*, and x this normalization term becomes

$$x = \sum_{\sigma,n=0}^{\infty}\frac{1}{\exp\left\{t\left[A\left(n + \frac{1}{2}\right)\frac{1}{x} + \frac{1}{2}\sigma\frac{1}{x} - \mu^*\right]\right\} + 1}. \tag{29}$$

The number of full Landau bands, for the first case $\varepsilon^{\downarrow}_{n_F} \leqslant \mu \leqslant \varepsilon^{\uparrow}_{n_F}$, is $n'_F - 1$, so that Eq. (29) becomes

$$x = 2(n_F' - 1) + \frac{1}{\exp\left\{ t\left[A\left(n_F' - \frac{1}{2} \right)\frac{1}{x} + \frac{1}{x} - \mu^* \right] \right\} + 1} + \frac{1}{\exp\left\{ t\left[A\left(n_F' - \frac{1}{2} \right)\frac{1}{x} - \frac{1}{x} - \mu^* \right] \right\} + 1}. \quad (30)$$

Here $n' = n+1$. Introducing the definitions $s = x - 2(n_F' - 1)$ and $\zeta = t/x$, Eq. (30) becomes

$$s = \frac{1}{y\exp(\zeta) + 1} + \frac{1}{y\exp(-\zeta) + 1}, \quad (31)$$

where

$$y = \exp\left\{ t\left[A\left(n_F' - \frac{1}{2} \right)\frac{1}{x} - \mu^* \right] \right\}. \quad (32)$$

We arrive at a simple algebraic equation of second order:

$$y^2 + 2y\left(1 - \frac{1}{s} \right)\cosh(\zeta) + 1 - \frac{2}{s} = 0. \quad (33)$$

The solution of this quadratic equation for $y > 0$ is

$$y = -\left(1 - \frac{1}{s} \right)\cosh(\zeta) + \left[\left(1 - \frac{1}{s} \right)^2 \cosh^2(\zeta) - \left(1 - \frac{2}{s} \right) \right]^{1/2}, \quad (34)$$

and, replacing y the chemical potential, Eq. (32), we obtain

$$\mu^* = A\left(n_F + \frac{1}{2} \right)\frac{1}{x} - \frac{1}{t}\ln\left\{ \frac{1-s}{s}\cosh\frac{t}{x} + \left[\left(\frac{1-s}{s} \right)^2 \cosh^2\frac{t}{x} + \frac{2-s}{s} \right]^{1/2} \right\}, \quad (35)$$

$$(36)$$

where $s = x - 2n_F$. Based on those definitions n_F can be calculated: if $2n_F + 1 \leqslant x \leqslant 2(n_F + 1)$, then $\varepsilon_{n_F}^{\downarrow} \leqslant \mu \leqslant \varepsilon_{n_F}^{\uparrow}$.

For example, if $1 \leqslant x \leqslant 2$, then $\varepsilon_0^{\downarrow} \leqslant \mu \leqslant \varepsilon_0^{\uparrow}$—therefore, $n_F = 0$—and if $3 \leqslant x \leqslant 4$, then $\varepsilon_1^{\downarrow} \leqslant \mu \leqslant \varepsilon_1^{\uparrow}$—therefore, $n_F = 1$.

x counts the full subbands $\sigma = \uparrow$ and $\sigma = \downarrow$. So $x/2 - 1 \leqslant n_F \leqslant (x-1)/2$.

In the second case, when $\varepsilon_{n_F}^{\downarrow} \leqslant \mu \leqslant \varepsilon_{(n_F+1)}^{\uparrow}$, Eq. (29) becomes

$$x = 2(n_F' - 1) + 1 + \frac{1}{\exp\left\{ t\left[A\left(n_F' + \frac{1}{2} \right)\frac{1}{x} - \frac{1}{x} - \mu^* \right] \right\} + 1} + \frac{1}{\exp\left\{ t\left[A\left(n_F' - \frac{1}{2} \right)\frac{1}{x} + \frac{1}{x} - \mu^* \right] \right\} + 1}. \quad (37)$$

Introducing $y = \exp\{t[A(n_F')(1/x) - \mu^*]\}$, $s' = x - 2n_F' + 1$ and $\eta = (A/2 - 1)t/x$, we rewrite Eq. (37) as

$$s' = \frac{1}{y\exp(\eta) + 1} + \frac{1}{y\exp(-\eta) + 1} \quad (38)$$

or

$$y^2 + 2y\left(1 - \frac{1}{s'} \right)\cosh(\eta) + 1 - \frac{2}{s'} = 0. \quad (39)$$

Taking the solution for $y > 0$,

$$y = \left(\frac{1}{s'} - 1 \right)\cosh(\eta) + \left[\left(\frac{1}{s'} - 1 \right)^2 \cosh^2(\eta) + \left(\frac{2}{s'} - 1 \right) \right]^{1/2}, \quad (40)$$

and substituting y via the chemical potential we obtain

$$\mu^* = A(n_F + 1)\frac{1}{x} - \frac{1}{t}\ln\left\{ G\cosh\left(\frac{A't}{x} \right) + \left[G^2\cosh^2\left(\frac{A't}{x} \right) + \frac{2 - s'}{s'} \right]^{1/2} \right\}. \quad (41)$$

$$(42)$$

Here $s' = x - (2n_F + 1)$, $G = (1 - s')/s'$, and $A' = A/2 - 1$. If $2(n_F + 1) \leqslant x \leqslant 2n_F + 3$, then $\varepsilon_{n_F}^{\downarrow} \leqslant \mu \leqslant \varepsilon_{(n_F+1)}^{\uparrow}$.

In Fig. 2 the chemical potentials, Eqs. (35) and (41), are plotted as a function of inverse magnetic field at $T = 1$ K. The chemical potential oscillates with the field. Sharp discontinuities are well emphasized at low temperatures. These discontinuities arise due to the presence of gaps in the electron energy spectrum. The discontinuity occurs at $x = 1, 3, \ldots$ and $x = 2, 4, \ldots$ as μ^* crosses the energy gap between two Landau levels and between two spin-split levels of the same Landau levels, respectively. The amplitude of discontinuity at even and odd integer values of x is proportional to the energy gap between two Landau levels, $\hbar\omega_c$, and the electron Zeeman splitting, $\hbar\omega_z$, respectively.

IV. ELECTRONIC PART OF THE TRANSITION RATE

In order to investigate the field dependence of the relaxation time T_1, Eq. (27), we consider below, as an example, the electronic properties of the magnetic impurity in GaAs quantum wells. It is known[26] that the resonance d level of TM impurities in a neutral state with configuration $3d^n$ always arises below the bottom of the conduction band. The

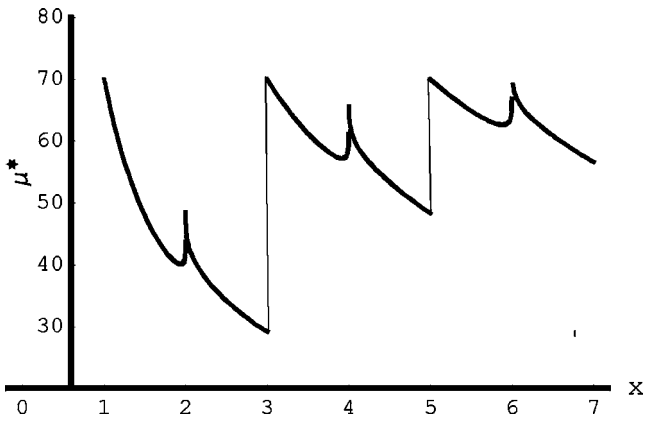

FIG. 2. The inverse field dependence of the dimensionless chemical potential is ploted for $T=1$ K. x is the number of full Landau subbands. The chemical potential oscillates with sharp discontinuities due to the presence of gaps in the electron energy spectrum.

crystal field acting on the impurity electron splits the d level into the $\gamma\nu=t_2$ or e states of a 3D crystal point group [we assume that the potential $V(z)$, responsible for the z confinement, forms a wide well which does not disturb the crystalline environment of the impurity cell]. Only the orbitals $|e1\rangle \propto |r^2-3z^2\rangle \sim Y_{20}$ are strongly hybridized with the Landau states.[23] Therefore we are left with the $\gamma\nu=e(u)$ wave function.

In the case of charged impurity states $3d^{n+1}$, however, the bare e level may appear very close to the bottom of the conduction band. For example, vanadium impurity V^{2+} in GaAs possesses just this kind of spectrum.[27] In some cases (e.g., Cr in GaAs) the e state of the charged impurity may appear above the bottom of the conduction band,[26] and this is the case of a strong resonance scattering, leading to a shift of the levels E_{bn} downward [dashed line in Fig. 1(a) (Ref. 23)].

There are three limits for this state to hybridize with the Landau electron states. The three examples of spin splitting illustrated by Fig. 3 in Ref. 23 show the variety of possibilities for bound states. The weak-scattering limit is presented in Fig. 3(a).[23] In this case the deep d level $\varepsilon_{ie\downarrow}$ is situated deeply below the first Landau subband. In this limit the localized Landau states $E_{i\sigma}^{(b)}$ are of the antibonding type. In the case when the Landau level E_b and the impurity level $\varepsilon_{ie\downarrow}$ are nearly degenerate, Fig. 3(b),[23] it causes strong resonance scattering for $\downarrow$ states. The strong resonance scattering limit for $\downarrow$ states occurs also when the impurity level $\varepsilon_{ie\downarrow}$ is within the Landau subbands. In this case the localized Landau states $E_{i\sigma}^{(b)}$ change character from bonding to antibonding type, depending on the impurity level position.

Since the influence of the TM impurity on Landau levels is *spin selective*, one should take into account the fact that the resonance states have a definite configuration of electron spins.[26] Let us consider, for example, the state of a TM impurity in a configuration d^n where the last (nth) electron occupies the bonding level $E_{ie\sigma}^{(b)}$.[23] Then the many-electron state of the $3d$ shell may be represented as $d^n=(ne_\uparrow^{r_1}e_\downarrow^{r_2}t_{2\uparrow}^{r_3}t_{2\downarrow}^{r_4})$ where $\Sigma_i r_i=n$ ($\downarrow$ and $\uparrow$ are two projections of the electron spin). Normally, TM ions in a crystal field of III-V semiconductors exist in the so-called high-spin state, which means that the $t_{2\sigma}$ and e_σ states are occupied in accordance with the Hund rule. Therefore, the spins of the e electrons in the $3d^n$ ions with $n\leqslant 5$ (from Ti to Mn) are directed parallel to the external field **B**. These electrons form the deep energy levels $E_{ie\uparrow}(d^n/d^{n-1})$ well below the bottom of the conduction band. The notation (d^n/d^{n-1}), commonly accepted in the spectroscopy of deep d states in semiconductors,[26,28–30] means that the occupation of the level $E_{i\gamma\sigma}(d^n/d^{n-1})$ corresponds to a change of the atomic configuration from d^{n-1} to d^n due to a transfer of a host spin σ electron to a γ state of the impurity $3d$ shell. The levels $E_{ie\downarrow}$ are more shallow, so that $E_b-E_{ie\uparrow} \gg E_b-E_{ie\downarrow}$. Filling these levels begins when the $3d$ shell is more than half-filled ($n>5$, the elements from Fe to Ni). In this case both the $E_{ie\uparrow}$ and $E_{ie\downarrow}$ levels are deep below the bottom of the conduction band, and the resonance scattering is weak.

As a result, one can expect that the effect of the resonance scattering will be strong for light elements (Ti, V, Cr, Mn) and resonance interaction splits the $m=0$ states predominantly from the down-spin Landau subband, whereas the potential scattering is spin independent.

We confine ourselves to the two-level approximation, so that the wave functions become

$$\Phi_{i\sigma}^{b}=\cos\,\theta_\sigma\varphi_{ie\sigma}+\sin\,\theta_\sigma\varphi_{b\sigma}, \tag{43}$$

$$\Phi_{i\sigma}^{a}=-\cos\,\theta_\sigma\varphi_{b\sigma}+\sin\,\theta_\sigma\varphi_{ie\sigma}, \tag{44}$$

with the mixing coefficient given by

$$\tan 2\theta_\sigma=\frac{2V_{eb}}{\Delta_\sigma}, \tag{45}$$

where V_{eb} is the hybridization matrix elements:

$$V_{eb}=\int d\mathbf{r}\varphi_{e1}(\mathbf{r})V_d(\mathbf{r})\varphi_b(\xi;E_{bn})\chi_0(z). \tag{46}$$

Here $\Delta_\sigma=E_b-\varepsilon_{e\sigma}$, φ_{e1} is the atomic d orbital that forms the "core" of the impurity wave function that retains its 3D character, because its radius r_d is small in comparison with the width of the well $V(z)$ responsible for the confinement in the z direction. φ_b is the wave function s for the bound Landau states with $m=0$. The spectrum and wave functions of these states were calculated in Ref. 21. The wave functions $\varphi_b(\xi;E_{bn})$ decaying at $\xi\to\infty$ describe the tail solution of the bound states,

$$\varphi_b(\xi,E_{bn})=\frac{\Gamma\left(\frac{1}{2}-\alpha_n\right)}{\sqrt{2\pi\psi\left(\frac{1}{2}-\alpha_n\right)}}\frac{W_{\alpha_n,0}(\xi)}{l_B\xi^{1/2}}. \tag{47}$$

Here $\xi=\frac{1}{2}(\rho/l_B)^2\alpha_n=\frac{1}{2}(1-\epsilon_{bn}l_B^2)$, $\epsilon_{bn}=2m_\perp E_{bn}/\hbar^2$, $W_{\alpha_n,0}(\xi)$ is the Whittaker function, and ρ is the radius from the impurity site. The energy levels ϵ_{bn} split from the corresponding Landau levels ϵ_{n0}.

Now we are using Eq. (44) to calculate the matrix elements of the hyperfine interaction, $S_{e1}^{n''\downarrow,n\uparrow}$, Eq. (13), and of

the electron phonon coupling, $A_{\Gamma M}^{n',ne1\sigma}$, Eq. (7). Since both interactions are mostly within the impurity crystalline cell the dependence of its matrix elements on the indices of the Landau states is very weak and we neglect it for the sake of simplicity. The obtained Fermi contact term

$$S_{e1}^{n''\downarrow,n\uparrow} = \langle \Phi_{ie1}^{(n'')\downarrow} | \delta(\mathbf{r}) | \Phi_{ie1}^{(n)\uparrow} \rangle \tag{48}$$

$$= \cos\theta_\uparrow \cos\theta_\downarrow \langle \varphi_{b\downarrow}^{(n'')} | \delta(\mathbf{r}) | \varphi_{b\uparrow}^{(n)} \rangle + \sin\theta_\uparrow \sin\theta_\downarrow \langle \varphi_{ie\downarrow} | \delta(\mathbf{r}) | \varphi_{ie\uparrow} \rangle \tag{49}$$

has a contribution from the spin density at the impurity nucleus composed of the core and tail contributions. The contribution from the integral on the core part, $|\varphi_{ie}(0)|^2 = \delta\rho(0)$, was calculated.[31] Since the tail part is an s function, then it is approximately given by

$$\langle \varphi_{b\downarrow}^{(n'')} | \delta(\mathbf{r}) | \varphi_{b\uparrow}^{(n)} \rangle \tag{50}$$

$$\simeq \delta\rho(0) \int_0^{\xi_d} \frac{W_{\alpha_{n''},0}(\xi) W_{\alpha_n,0}(\xi)}{\xi} d\xi \simeq \delta\rho(0)\xi_d, \tag{51}$$

where $\xi_d = \frac{1}{2}(r_d/l_B)^2$ which is the overlap of the tail part on the impurity site multiplied by the spin density at the impurity, $\delta\rho(0)$, which is contributed by the s orbital. This approximation does not affect the magnetic field or the temperature dependence of the relaxation rate T^{-1} which is retained in the term ξ_d. Therefore the Fermi contact, Eq. (48), becomes

$$S_{e1}^{n''\downarrow,n\uparrow} = \cos\theta_\uparrow \cos\theta_\downarrow \delta\rho(0)(\tan\theta_\uparrow \tan\theta_\downarrow + \xi_d). \tag{52}$$

Similarly to the hyperfine interaction, the matrix elements for the electron phonon interaction $A_{\Gamma M}^{n',ne1\sigma}$, Eq. (7), are composed of two contributions:

$$A_{\Gamma M}^{n',ne1\sigma} = (\cos^2\theta_\sigma A_{\Gamma M,b}^{n'n\sigma} + \sin^2\theta_\sigma A_{\Gamma M}^{e1,e1}), \tag{53}$$

where the tail and core parts, respectively, are $A_{\Gamma M,b}^{n'n\sigma} = (1/\alpha_\Gamma)\langle \varphi_{b\sigma}^{(n')} | V_{\Gamma M}(\mathbf{r}) | \varphi_{b\sigma}^{(n)} \rangle$ and $A_{\Gamma M}^{e1,e1} = (1/\alpha_\Gamma)\langle \varphi_{ie\sigma} | V_{\Gamma M}(\mathbf{r}) | \varphi_{ie\sigma} \rangle$.

Neglecting the index dependence of matrix elements Eq. (53) becomes

$$A_{\Gamma M}^{e1,e1\sigma} = (\cos^2\theta_\sigma A_{\Gamma M,b}^{\sigma} + \sin^2\theta_\sigma A_{\Gamma M}^{e1,e1}). \tag{54}$$

Here $A_{\Gamma M}^{e1,e1}$ is the energy interaction of the d electron with the localized vibration and is known as the Jahn-Teller interaction (except for the A_1 mode). $A_{\Gamma M,b}^{\sigma}$ is the energy interaction due to the tail wave function with the localized vibration. Since the localized mode acts mainly in the intersite cell with radius of localization of the impurity, r_d, we can write

$$A_{\Gamma M,b}^{\sigma} \simeq A_{\Gamma M} \int_0^{\xi_d} \frac{W_{\alpha_{n''},0}(\xi) W_{\alpha_n,0}(\xi)}{\xi} d\xi \simeq A_{\Gamma M}\xi_d. \tag{55}$$

The electron phonon interaction becomes

$$A_{\Gamma M}^{e1,e1\sigma} = \cos^2\theta_\sigma (A_{\Gamma M,b}\xi_d + \tan^2\theta_\sigma A_{\Gamma M}^{e1,e1}). \tag{56}$$

Assuming the force constant in the intersite cell acting on the impurity to be equal for both the impurity and Landau electron, $A_{\Gamma M,b} = A_{\Gamma M}^{e1,e1} = A_{\Gamma M}$, Eq. (56) can be written as

$$A_{\Gamma M}^{e1,e1\sigma} = \cos^2\theta_\sigma A_{\Gamma M}(\xi_d + \tan^2\theta_\sigma). \tag{57}$$

One can see that the tail part can interact with all vibrational modes while the d-electron state of the impurity in the T_d symmetry site can be coupled to the vibrational modes of A_1, E, and T_2 symmetry. The localized state $|e1\rangle$ can interact only with the vibrational modes $\Gamma M = E(u)$ and $A_1(a_1)$ vibration modes. Therefore the contribution of the dimensionless tensor comes from the nonzero elements $\rho_{e1,e1}^{Eu} = -1/\sqrt{2}$ and $\rho_{e1,e1}^{A_1 a_1} = 1/\sqrt{2}$.[35]

Inserting Eqs. (52) and (57) into the matrix elements $R_{\Gamma M\sigma}^{\lambda'\lambda''\lambda}$ Eq. (12) yields

$$R_{\Gamma M\downarrow} = \frac{1}{2}\cos^6\theta_\downarrow \cos^2\theta_\uparrow A_{\Gamma M}^2(\xi_d + \tan^2\theta_\downarrow)^2 \tag{58}$$

$$\times \delta\rho^2(0)(\tan\theta_\uparrow \tan\theta_\downarrow + \xi_d)^2 \tag{59}$$

for channel A and

$$R_{\Gamma M\uparrow} = \frac{1}{2}\cos^6\theta_\uparrow \cos^2\theta_\downarrow A_{\Gamma M}^2(\xi_d + \tan^2\theta_\uparrow)^2 \tag{60}$$

$$\times \delta\rho^2(0)(\tan\theta_\uparrow \tan\theta_\downarrow + \xi_d)^2 \tag{61}$$

for channel B. Now we are in the position to present the behavior of the transition rate $W(T_1)$ for the weak- and strong-scattering limits.

V. WEAK-SCATTERING LIMIT

In order to present an implicit behavior of $W(T_1)$ we apply this result to the case of the weak-scattering limit—i.e., $\tan\theta_\sigma \approx V_{eb}/\Delta_\sigma$. For presenting the magnetic field dependence of $W(T_1)$ we use the estimation $|V_{eb}|^2 = |V_d|^2\xi_d$ where V_d is the hybridization energy of the impurity. The Fermi contact interaction, Eq. (52), becomes

$$S_{e1}^{n''\downarrow,n\uparrow} = \delta\rho(0)(1 + \eta_{\uparrow\downarrow})\xi_d, \tag{62}$$

and the electron phonon interaction, Eq. (57), becomes

$$A_{\Gamma M}^{e1,e1\sigma} = A_{\Gamma M}(1 + \eta_\sigma)\xi_d, \tag{63}$$

where $\eta_\sigma = |V_d|^2/\Delta_\sigma\Delta_\sigma$.

The matrix elements, Eqs. (59) and (61), become

$$R_{\Gamma M\sigma} = \frac{1}{2}[A_{\Gamma M}(1 + \eta_\sigma)]^2[\delta\rho(0)(1 + \eta_{\uparrow\downarrow})]^2\xi_d^4 \tag{64}$$

and can be written as

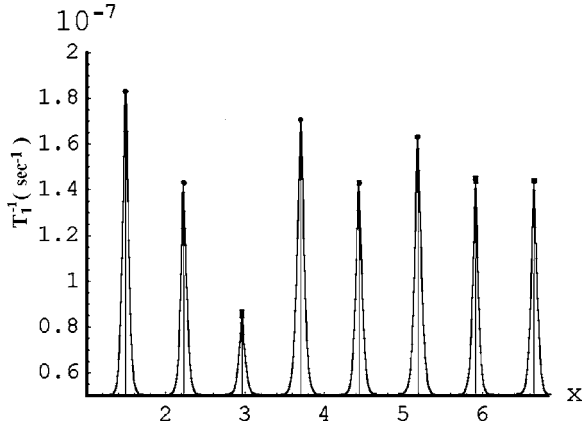

FIG. 3. The field dependence of the NSR (nuclear spin relaxation) rate for the case of weak-scattering limit for the temperature of $T=20$ K. The points represent the only allowed transitions. The resonance spikes are equidistant and depend on the frequency of the localized phonon. x is the number of full Landau subbands.

$$\sum_{\sigma} R_{\Gamma M\sigma} \tag{65}$$

$$=\frac{1}{2x^4}\delta\rho^2(0)A_{\Gamma M}^2 n_i^4(1+\eta_{\uparrow\downarrow})^2[(1+\eta_{\uparrow\uparrow})^2+(1+\eta_{\downarrow\downarrow})^2], \tag{66}$$

where $n_i=\pi r_d^2\tilde{n}$ is the 2D electron density on the impurity site. Inserting Eq. (65) into Eq. (27) the transition rate becomes

$$W(T_1)=D\sum_{\Gamma Mnn'}\frac{I_{\Gamma M}}{x\sinh\frac{\beta}{2}\hbar\omega_\Gamma\left[\cosh f_\Gamma(x)+\cosh\frac{\beta}{2}(\hbar\omega_\Gamma)\right]}, \tag{67}$$

$$I_{\Gamma M}=\frac{1}{2}n_i^4A_{\Gamma M}^2\delta\rho^2(0)(1+\eta_{\uparrow\downarrow})^2[(1+\eta_{\uparrow\uparrow})^2+(1+\eta_{\downarrow\downarrow})^2], \tag{68}$$

provided the final state n' satisfies Eq. (23).

As an example we apply this result to Fe impurity in GaAs, which is known to produce an acceptor level $E_{ie\downarrow}(d^6/d^5)$ well below the bottom of the conduction band.[26,34] The gaps $\Delta_\uparrow$ and $\Delta_\downarrow$ are, therefore, of the order of 1 eV. The hybridization parameter normally does not exceed 0.2 eV. In this case of the weak-scattering limit η_σ can be neglected.

Choosing the mode symmetry of the localized phonon to be $\Gamma M=Eu$ two frequencies are possible: $\hbar\omega_E^A=85$ cm^{-1} and $\hbar\omega_E^0=260$ cm^{-1} for the acoustical and optical modes, respectively.[32] The acoustical phonon is the dominant mode, so we will consider it here. The coupling to acoustic phonons turns out to be of intermediate strength.[33]

We plot in Fig. 3 a quantitative picture of T_1^{-1} for the nuclear spin of the Fe impurity. The calculation is done assuming the spin density $\delta\rho(0)=0.22$ a.u.$^{-3}$,[31] and phonon frequency $\hbar\omega_E^A=85$ cm^{-1}.[32] In this figure the spikes represent the NSR rate T_1^{-1} as a function of inverse field, x, for $T=20$ K. In the intervals between the spikes, T_1^{-1}, almost vanish since the spin-flip transitions are allowed energetically only for discrete values of the magnetic field satisfying Eq. (23). These spikes may appear above the NSR rate background caused by the continuous part of the electron-phonon interaction which was not considered here.

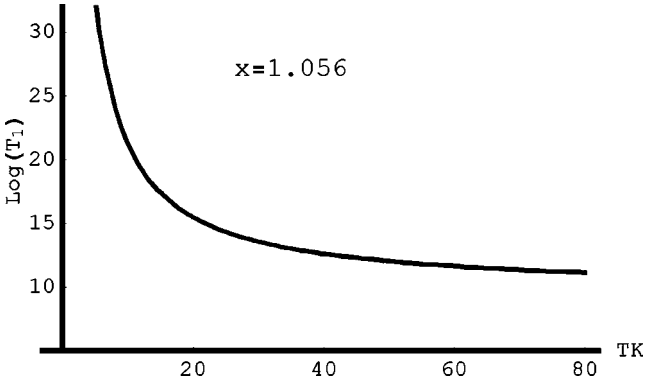

FIG. 4. The temperature dependence of T^{-1} at $x=1.056$ is plotted. The difference between its behavior at low temperatures from that at high temperature arises from the thermal excitation of the localized phonons.

The obtained NSR rate T_1^{-1} oscillates periodically in the inverse magnetic field due to the chemical potential oscillation with the field. The passage from minimum to maximum is reached as μ^* crosses the Landau gap into the spin splitting gap; see Eq. (35). The same behavior but with small amplitude arises as μ^* crosses the spin splitting into the gap between two Landan levels (LL's); see Eq. (41). This oscillation structure is superimposed onto the linear in the magnetic field background.

The resonance spikes are placed at equal distance depending on the frequency of the localized phonon.

In the Fig. 4 we plot T_1 as a function of temperature for $x=1.056$. The temperature dependence of T_1 at low temperatures differs from that at high temperature. This difference arises from the thermal excitation of the localized phonons. For instance, at low temperatures $k_BT\ll\hbar\omega_E^A$ the NSR time varies exponentially, $T_1\propto\exp(\hbar\omega_E^A/k_BT)$. At high temperature $k_BT>\hbar\omega_E^A$ the NSR time decreases as $T_1\propto 1+\hbar\omega_E^A/k_BT$ in an asymptotic form. It is clear that for high temperature the multiphonon process becomes dominant.

VI. STRONG-SCATTERING LIMIT

We calculate here the behavior of $W(T_1)$ for the case of the strong-scattering limit—i.e., $\Delta_\downarrow\ll V_{eb}$ and $V_{eb}\ll\Delta_\uparrow$. In this limit we are using in the matrix elements the following approximations: $\cos\theta_\downarrow\simeq\sqrt{\frac{1}{2}+\Delta_\downarrow/V_{eb}}$, $\cos\theta_\uparrow\simeq\sqrt{1-V_{eb}/\Delta_\uparrow}$, $\sin\theta_\downarrow\simeq\sqrt{\frac{1}{2}-\Delta_\downarrow/V_{eb}}$, and $\sin\theta_\uparrow\simeq V_{eb}/\Delta_\uparrow$. Hence Eq. (52) for the Fermi contact term becomes

$$S_{e1}^{n''\downarrow,n\uparrow}\simeq\frac{1}{\sqrt{2}}\delta\rho(0)(\xi_d+\sqrt{\eta_{\uparrow\uparrow}\xi_d}). \tag{69}$$

The electron-phonon interaction terms, Eq. (57), become

$$A_{\Gamma M}^{e1,e1\downarrow} \simeq \frac{1}{2} A_{\Gamma M}(\xi_d + 1), \tag{70}$$

$$A_{\Gamma M}^{e1,e1\uparrow} \simeq A_{\Gamma M}\xi_d(1 + \eta_{\uparrow\uparrow}). \tag{71}$$

Since $\xi_d \ll 1$, then $A_{\Gamma M}^{e1,e1\uparrow} \ll A_{\Gamma M}^{e1,e1\downarrow}$ and therefore $R_{\Gamma M\uparrow}$, Eq. (61), can be neglected and only channel A is dominant. The matrix elements, Eq. (59), become

$$R_{\Gamma M\downarrow} = \frac{1}{16} A_{\Gamma M}^2 \delta\rho^2(0)(\xi_d^2 + 2\sqrt{\eta_{\uparrow\uparrow}}\xi_d^{3/2} + \eta_{\uparrow\uparrow}\xi_d). \tag{72}$$

Under these conditions the relaxation rate, Eq. (27), becomes

$$W(T_1) = \frac{D}{16} \tag{73}$$

$$\times \sum_{\Gamma Mnn'} \frac{A_{\Gamma M}^2 \delta\rho^2(0)(n_i \eta_{\uparrow\uparrow} x^2 + 2n_i^{3/2}\sqrt{\eta_{\uparrow\uparrow}} x^{3/2} + n_i^2 x)}{\sinh \frac{\beta}{2}\hbar\omega_\Gamma \left[\cosh f_\Gamma(x) + \cosh \frac{\beta}{2}(\hbar\omega_\Gamma) \right]}. \tag{74}$$

Since n_i, the electron density per impurity atom for a typical concentration of $10^{11}-10^{12}$ cm^{-2}, is very small, only the leading term is left:

$$W(T_1) = D \sum_{\Gamma Mnn'} \frac{I_{\Gamma M} x^2}{\sinh \frac{\beta}{2}\hbar\omega_\Gamma \left[\cosh f_\Gamma(x) + \cosh \frac{\beta}{2}(\hbar\omega_\Gamma) \right]}, \tag{75}$$

where

$$I_{\Gamma M} = \frac{1}{16} A_{\Gamma M}^2 \delta\rho^2(0) n_i \eta_{\uparrow\uparrow}. \tag{76}$$

To compare the results of the strong- and weak-scattering limits we are using the same Fe impurity in GaAs but with the energy position of the impurity, $\varepsilon_{e\downarrow}$, close to the conduction band. With the present choice of parameters we plot in Fig. 5 a quantitative picture of T_1^{-1}, Eq. (75), for the nuclear spin of the Fe impurity. The calculation is done by using the same details as mentioned in the former section. Unlike the case of the weak-scattering limit here the oscillations of the spikes in the NSR rate T_1^{-1} are suppressed by a strong field dependence. Here T_1^{-1} fastly increases with a quadratic power of x.

The temperature dependence of T_1^{-1} is the same as in the case of the weak-scattering limit. The behavior in this case is qualitatively as in Fig. 4 but with a larger relaxation time.

VII. CONCLUSION

The temperature and field dependence of the localized phonon-assisted nuclear spin relaxation rate was calculated in detail for the case of weak- and strong-scattering limits in a 2DEG with magnetic impurities under a strong magnetic field. It was found that only resonant transitions are allowed to occur with equal magnetic field intervals, which depends on the vibrational mode frequency. This spectral structure can be used as a probe for studying the localized vibrational-mode frequency, the electron-phonon coupling for various transition-metal impurities, and pecularities of hyperfine interactions in these systems. Our calculations show that the NSR of the magnetic impurity in our system is enhanced by a few orders of magnitude compared to that in bulk semiconductors.[31]

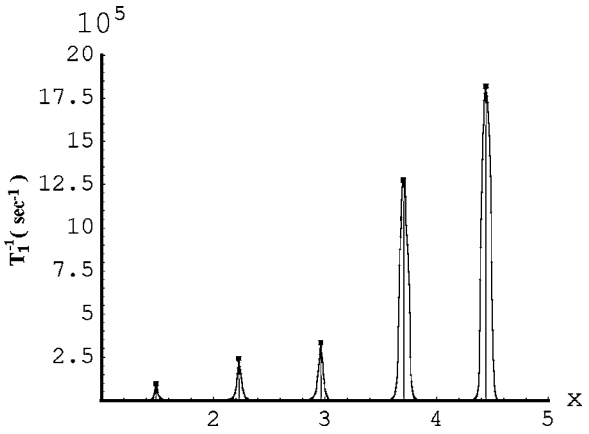

FIG. 5. The field dependence of the NSR rate in the case of the strong-scattering limit at the temperature of $T=20$ K. The points represent the only allowed transitions. x is the number of full Landau subbands.

Our results indicate that the nuclear spin relaxation rate of the impurity might be controlled by the impurity element—i.e., the position of the resonance d level of the impurity, $E_{ie\sigma}$—and also by the electron density in the impurity site, n_i. In the weak-scattering limit we have got approximately $T_1 \sim 10^7$ s. The same parameter used for the case of the strong-scattering limit leads us to a much shorter relaxation time $T_1 \sim 10^{-5}$ s. We have here the usual situation when the theory cannot give any reliable estimates for the relaxation time due to its extreme sensitivity to the position of the resonance d level of the impurity in the gap, $E_{ie\sigma}$. On the other hand, these results show that the relaxation time T_1 may vary by orders of magnitude within reasonable values of the parameters.

Yet another aspect of the localized phonon-assisted resonant nuclear-electron spin flip is a possibility of selective manipulation of nuclear spin qubits in the emerging field of spin-based quantum memory and computation devices. Because of the very long nuclear relaxation time T_1 the nuclear spins could be considered as the best suitable candidates for a qubit.[19] The main ingredients of such a prototype system are nuclear *spin qubits*, coupled through the hyperfine interaction to a phase-coherent electron spin system in a nanostructure[18] or in a quantum Hall effect system.[19]

The resonant nature of the magnetic field dependence of T_1^{-1} in these systems may be the solution for manipulating the qubits with exponential precision.

*Electronic address: p.dahan@ruppin.ac.il

[1] K. von Klitzing, G. Dorda, and M. Pepper, Phys. Rev. Lett. **45**, 494 (1980); D. C. Tsui, H. L. Störmer, and A. C. Gossard, *ibid.* **48**, 1559 (1982); R. B. Laughlin, *ibid.* **50**, 1395 (1983); *Perspectives in Quantum Hall Effect*, edited by S. Das Sarma and A. P. Pinczuk (Wiley, New York, 1997).

[2] I. D. Vagner and T. Maniv, Phys. Rev. Lett. **61**, 1400 (1988); see for a recent review I. D. Vagner, *HAIT J. Sci. Eng.* 1, 152 (2004).

[3] S. E. Barrett, R. Tycko, L. N. Pfeiffer, and K. W. West, Phys. Rev. Lett. **72**, 1368 (1994); R. Tycko, S. E. Barrett, G. Dabbagh, L. N. Pfeiffer, and K. W. West, Science **268**, 1460 (1995); N. N. Kuzma, P. Khandelwal, S. E. Barrett, L. N. Pfeiffer, and K. W. West, *ibid.* **281**, 5377 (1999); J. N. Smet, R. A. Deutschmann, F. Ertl, W. Wegscheider, G. Abstreiter, and K. von Klitzing, Nature (London) **415**, 281 (2002).

[4] I. D. Vagner, A. S. Rozhavsky, P. Wyder, and A. Yu. Zyuzin, Phys. Rev. Lett. **80**, 2417 (1998); V. A. Cherkasskiy, S. N. Shevchenko, A. S. Rozhavsky, and I. D. Vagner, Low Temp. Phys. **25**, 541 (1999).

[5] Yu. V. Pershin, S. N. Shevchenko, I. D. Vagner, and P. Wyder, Phys. Rev. B **66**, 035303 (2002); V. Fleurov, V. A. Ivanov, F. M. Peeters, and I. D. Vagner, Physica E (Amsterdam) **14**, 361 (2002).

[6] Y. B. Lyanda-Geller, I. L. Aleiner, and B. L. Altshuler, Phys. Rev. Lett. **89**, 107602 (2002).

[7] See for a recent review J. Schliemann, A. Khaetskii, and D. Loss, J. Phys.: Condens. Matter **15**, R1809 (2003).

[8] I. V. Lerner and Yu. E. Lozovik, Sov. Phys. JETP **51**, 588 (1980).

[9] Yu. A. Bychkov, S. V. Iordanskii, and G. M. Eliashberg, Pis'ma Zh. Eksp. Teor. Fiz. **33**, 152 (1981) [JETP Lett. **33**, 143 (1981)].

[10] C. Kallin and B. I. Halperin, Phys. Rev. B **30**, 5655 (1984).

[11] D. H. Lee and C. L. Kane, Phys. Rev. Lett. **64**, 1313 (1990); S. L. Sondhi, A. Karlhede, S. A. Kivelson, and E. H. Rezayi, Phys. Rev. B **47**, 16419 (1993); Yu. A. Bychkov, T. Maniv, and I. D. Vagner, *ibid.* **53**, 10148 (1996).

[12] C. P. Slichter, *Principles of Magnetic Resonance*, 3rd ed. (Springer-Verlag, Berlin, 1991).

[13] See for a review M. I. Dyakonov and V. I. Perel, in *Modern Problems in Condensed Matter Sciences*, edited by F. Meier and B. P. Zakharchenya (North-Holland, Amsterdam, 1984), Vol. 8, p. 11.

[14] R. G. Mani, W. B. Johnson, V. Narayanamurti, V. Privman, and Y.-H. Zhang, Physica E (Amsterdam) **12**, 152 (2002); J. M. Taylor, C. M. Markus, and M. D. Lukin, Phys. Rev. Lett. **90**, 206803 (2003).

[15] V. Privman, I. D. Vagner, and G. Kventsel, Phys. Lett. A **236**, 141 (1998).

[16] B. E. Kane, Nature (London) **393**, 133 (1998).

[17] I. Shlimak, V. I. Safarov, and I. D. Vagner, J. Phys.: Condens. Matter **13**, 6059 (2001).

[18] Yu. Pershin, I. D. Vagner, and P. Wyder, J. Phys.: Condens. Matter **15**, 997 (2003).

[19] See for a review V. Privman, D. Mozyrsky, and I. D. Vagner, Comput. Phys. Commun. **146**, 331 (2002).

[20] Ju. H. Kim, I. D. Vagner, and L. Xing, Phys. Rev. B **49**, 16777 (1994); S. I. Erlingsson, Y. V. Nazarov, and V. I. Fal'ko, *ibid.* **64**, 195306 (2001); Y. B. Lyanda-Geller, I. L. Aleiner, and B. L. Altshuler, Phys. Rev. Lett. **89**, 107602 (2002).

[21] Y. Avishai, M. Ya. Azbel, and S. A. Gredeskul, Phys. Rev. B **48**, 17280 (1993).

[22] S. A. Gredeskul, M. Zusman, Y. Avishai, and M. Ya. Azbel, Phys. Rep. **288**, 223 (1997).

[23] P. Dahan, V. Fleurov, K. Kikoin, and I. D. Vagner, Phys. Rev. B **65**, 165313 (2002).

[24] U. Lindefelt, Phys. Rev. B **28**, 4510 (1983).

[25] A. L. Natadze, A. Z. Ryskin, and B. G. Vekhter, in *Jahn-Teller Effects in Optical Spectra of II-VI and III-V Impurity Crystals*, edited by Yu. E. Perlin and M. Wagner (Elsevier, Amsterdam, 1984).

[26] K. A. Kikoin and V. N. Fleurov, *Transition Metal Impurities in Semiconductors* (World Scientific, Singapore, 1994).

[27] H. Katayama-Yoshida and A. Zunger, Phys. Rev. B **33**, 2961 (1986).

[28] V. I. Sokolov, Sov. Phys. Solid State **29**, 1061 (1987).

[29] A. Zunger, in *Solid State Physics*, edited by F. Seitz and D. Turnbull (Academic Press, New York, 1986), Vol. 39, p. 275.

[30] *Numerical Data and Functional Relationships in Science and Technology*, edited by O. Madelung, Landolt-Bornstein, New Series, Group III, Vol. 22, pt. 6 (Springer-Verlag, Berlin, 1989).

[31] H. Katayama-Yoshida, Int. J. Mod. Phys. B **1**, 1207 (1987).

[32] O. Mualin, E. E. Vogel, M. A. de Orue, L. Martinelli, G. Bevilacqua, and H. J. Schulz, Phys. Rev. B **65**, 35211 (2002).

[33] J. Rivera-Iratchet, M. A. de Orue, and E. E. Vogel, Phys. Rev. B **34**, 3992 (1986).

[34] Luiza M. R. Scolfaro and A. Fazzio, Phys. Rev. B **36**, 7542 (1987).

[35] F. G. Koster, J. O. Dimock, R. G. Wheeler, and H. Statz, *Properties of the Thirty-Two point Groups* (MIT Press, Cambridge, MA, 1963).